A consistent thermodynamic molecular model of n-hydrofluorolefins and blends for refrigeration applications

Carlos G. Albà,[†] Lourdes F. Vega[‡] and Fèlix Llovell,[†*]

[†]Department of Chemical Engineering and Materials Science. IQS School of Engineering, Universitat Ramon Llull, Via Augusta 390, 08017, Barcelona, Spain

[‡] Research and Innovation Center on CO_2 and H_2 (RICH), Center for Catalysis and Separation (CeCaS) and Chemical Engineering Department. Khalifa University. PO Box 127788, Abu Dhabi, UAE

*Corresponding author: E-mail: felix.llovell@iqs.edu, phone: +34 93 2670000

Abstract

This work presents a thermodynamic model that characterizes 4th-generation hydrofluoroolefins (HFOs)-based refrigerants with the molecular-based soft-SAFT equation of state (Blas and Vega, 1998) as well as its application in process simulations for a selected refrigeration application. The evaluation of the HFOs has been done building on a molecular model transferred from the equivalent hydrofluorocarbons (HFCs), taking advantage of the similarities between the two chemical families. The model has been used to calculate all thermophysical properties of the selected HFOs relevant for their application as refrigerants, including the saturated density, vapor pressure, heat capacity, speed of sound, surface tension and viscosity, providing good agreement with experimental available data. In addition, phase equilibria, interfacial behavior and viscosity calculations have been performed for blends between HFCs and the two most common HFOs, R1234yf and R1234ze. The obtained thermodynamic properties have been used for a process simulation of a vapor compression refrigeration system, comparing the 3rd generation refrigerant R410A with these 4th generation blends, including the Coefficient of Performance for different cases, in order to establish the best alternative to R410A. Overall, this work shows how molecular modeling tools can be used now a day, as a complementary tool to generate reliable data for process simulation, in this case related to the search for alternative refrigerants.

Keywords: Hydrofluorolefins, soft-SAFT, vapor-liquid equilibria, surface tension, viscosity, coefficient of performance.

Nomenclature

Abbreviations

AAD	Absolute Average Deviation
CPA	Cubic-Plus-Association
EoS(s)	Equation(s) of State
GWP	Global Warming Potential
HT	High Temperature
LJ	Lennard-Jones
LT	Low Temperature
PC	Perturbed-Chain
SAFT	Statistical Associating Fluid Theory
VLE	Vapor-liquid equilibrium

Latin symbols

A	Helmholtz free energy
B	Free-volume overlap viscosity parameter
g	Radial distribution function
k_B	Boltzmann constant
K^{HB}	Volume of association
L_v	Correlation length viscosity parameter
M_w	Molecular weight
m	Chain length
P	Pressure
R	Ideal gas constant
T	Temperature
V	Volume
x	Mole fraction

Greek symbols

α	Energy barrier viscosity parameter
ε	Energy parameter of the intermolecular LJ potential
η	Size parameter of the mixing rules
ρ	Density
σ	Size parameter of the LJ intermolecular potential
ξ	Energy parameter of the mixing rules

Superscripts

HB	hydrogen bonding
res	residual
ref	reference

Subscripts

α, β	association sites
B	Boltzmann
i, j	compound
r	reduced
w	weight

1. Introduction

Nowadays, there is an urgent need for the study and implementation of new refrigerants with reduced Global Warming Potential ($GWP_{100years}$ [1]) due to the negative impact into the environment of the ones in current use, the hydrofluorocarbons (HFCs). In an effort to mitigate climate change, international initiatives aiming at the reduction of HFCs emissions have been recently adopted. In this respect, EU Regulation No. 517/2014 (Schulz and Kourkoulas, 2014) established restrictions on placing on the market certain products and equipment based on the intended application and the GWP of the refrigerants to be used. Moreover, the Kigali's amendment to the Montreal's Protocol, signed by 197 countries in 2016, and entering into force in 2019, schedules an ambitious program to reduce the production and consumption of HFCs (Heath, 2017), aiming at avoiding up to 0.5 °C of warming by the end of the 21st century. Accordingly, some of the currently most employed HFC compounds and blends used in refrigeration and air conditioning, e.g., R134a (GWP=1430), R404A (GWP=3922) and R410A (GWP=2088), must be replaced in the short-term by environment friendly and energy efficient alternative refrigerants (Mota-Babiloni et al., 2017).

In the last decade, some 4th generation refrigerants have appeared as new candidates with a collection of adequate thermophysical properties, low GWP, a null ozone depletion potential (ODP), good chemical stability, low toxicity and acceptable flammability. McLinden et al. performed two studies (McLinden et al., 2017, 2014) where they identified, among a total of 1200 candidates, 28 low-GWP fluids as potential pure-fluid replacements for refrigeration systems (mainly focused on air conditioning). The largest group corresponded to hydrofluoroolefins (HFOs). It is estimated that approximately 13% of refrigerants in use in 2030 will be HFO-based, with an increasing market due to the legislation constraints applied over third generation HFCs refrigerants. In general, HFOs represent a realistic alternative due to their excellent environmental properties, although their relative high flammability prevents their use as single compounds from a safety perspective (Goetzler et al., 2014). At this stage, the most suitable option is the combination of both, the good environmental properties of HFOs with the no flammable and good thermodynamic properties of HFCs, in order to obtain an efficient refrigerant blend with a reduced GWP,

[1] Note that these numbers indicate the amount of heat trapped in the atmosphere by the gas up to a time horizon of a century and it is usually referred simply as GWP.

null ODP and low flammability at the same time. However, the range of compositions and mixture combinations is huge; consequently, time and resources are devoted to characterize the thermophysical properties of these blends in order to find the optimal combination for *ad-hoc* refrigeration applications. In this regard, theoretical tools, based either on molecular simulations or equations of state (EoSs), can provide great insight, offering a saving of time and costs, and guiding the experimental work towards the most promising options.

From one side, it is important to mention the development of new force fields to describe the interactions of HFOs using molecular simulations for phase equilibria (Raabe, 2019, 2016, 2015, 2013; Raabe and Maginn, 2010) and interfacial properties (Li et al., 2019). The reader is referred to some recent publications and reviews (Raabe, 2019, 2017, 2016), where the current stage of the force field development for HFOs and their applications is discussed in detail. From the other side, several authors have described HFOs and their mixtures using cubic and advanced EoSs. Fouad and Vega used the polar and perturbed chain statistical associating fluid theory (PC-SAFT) coupled with the density gradient theory (DGT) to predict the vapor–liquid equilibrium, isobaric heat capacity, speed of sound, and surface tension of selected HFC and HFO-based commercial azeotropic blends (Fouad and Vega, 2018a). They included a dipolar contribution in the model of these refrigerants, finding very good agreement between the model used and the available data using only one binary parameter. Other authors (Kang et al., 2018) used the PC-SAFT and Cubic Plus Association (CPA) EoSs to carry out an indepth analysis on the impact of the parameter estimation method on model development and validation for these compounds. These authors combined different thermodynamic properties to find the best approach to describe HFOs. They highlighted that PC-SAFT provided better results in correlating most of the second-order derivative properties containing speed of sound, isothermal compressibility and isobaric thermal expansivity, while CPA performed better in predicting isobaric heat capacity. They also recommended the use of vapor pressure and liquid density at low pressures as input experimental data for the parameters optimization. Very recently, Al Ghafri et al. (Al Ghafri et al., 2019) carried out an extensive study of the thermodynamic properties of R1234yf and R1234ze(E)) refrigerant mixtures combining experimental work and a Helmholtz energy model using the mixing rules provided by the GERG 2008 EoS.

In addition to these contributions, focused on thermodynamic properties, it is interesting to highlight the work of He and coworkers (He et al., 2015), who used the Free-Volume Theory on the evaluation of the viscosity for R1234yf and R1234ze(E) as a function

of temperature and density over a wide range conditions. They also studied several mixtures of these HFOs with R32. Finally, Fouad and Vega (Fouad and Vega, 2018b) evaluated the viscosity of HFC-HFO systems by implementing the entropy scaling approach coupled to PC-SAFT, obtaining excellent agreement with available experimental data.

The goal of this contribution is to provide a consistent thermodynamic model to describe the physicochemical behavior of 4th generation HFO-based refrigerants as low GWP alternatives to the current HFC-based refrigerants. For this purpose, the well-known soft-SAFT molecular-based EoS is used. Soft-SAFT (Blas and Vega, 1997) has been successfully applied to describe the thermodynamic properties of complex fluids and mixtures (Lloret et al., 2017; Llovell et al., 2015; Pàmies and Vega, 2001; Pedrosa et al., 2006; Vega et al., 2017; Vega and Llovell, 2016). The equation has been previously used to model perfluoroalkanes (Dias et al., 2009, 2004), fluorinated ionic liquids (Ferreira et al., 2019; Llovell et al., 2011; Pereiro et al., 2017) and hydrofluorocarbons (Llovell et al., 2013a; Vilaseca et al., 2010), offering an excellent performance for the three families. The work presented here belongs to a long-term project on using molecular-based models as a tool to characterize and predict the properties of new refrigerants and their blends.

2 Theory: soft-SAFT EoS

The soft-SAFT EoS (Blas and Vega, 1998, 1997) is one of the variants of the original SAFT EoS (Chapman et al., 1990). This equation explicitly accounts for hydrogen-bonding and other high-range directional (association) forces. It is written as a sum of contributions to the residual Helmholtz energy, A^{res}:

$$A^{res} = A - A^{id} = A^{ref} + A^{chain} + A^{assoc} \quad (1)$$

where the subscripts *id*, *ref*, *chain* and *assoc* refer to the ideal, reference, chain and association terms, respectively.

The reference term includes the repulsive and attractive interaction of the segments forming the chains. Soft-SAFT uses a Lennard-Jones (LJ) intermolecular potential through the equation of Johnson et al. (Johnson et al., 1993), characterized by the depth of the potential well, ε, and the diameter of the LJ sphere, σ. For mixtures, the same expression is employed by developing a pseudo pure fluid using the van der Waals 1-fluid theory. The crossed LJ characteristic parameters are obtained from:

$$\sigma_{ij} = \left(\frac{\sigma_{ii}+\sigma_{jj}}{2}\right) \tag{2}$$

$$\varepsilon_{ij} = \xi_{ij}\left(\varepsilon_{ii}\varepsilon_{jj}\right)^{1/2} \tag{3}$$

where i and j refer to the different components in the mixture. ξ_{ij} is the energy binary adjustable parameter (equivalent to k_{ij} in cubic EoSs).

The expressions for the chain and association terms, accounting for chain formation and site-site interaction, respectively, are directly written for mixtures as follows:

$$A^{chain} = RT\sum_i x_i(1-m_i)\ln g_R(\sigma_i) \tag{4}$$

$$A^{assoc} = RT\sum_i x_i\left[\sum_\alpha\left(\ln X_i^\alpha - \frac{X_i^\alpha}{2}\right)+\frac{M_i}{2}\right] \tag{5}$$

where T is the temperature, R is the ideal gas constant, R = $N_A k_B$, being k_B is the Boltzmann constant and N_A Avogadro's number, x_i is the mole fraction of molecules i in the system, m_i the chain length of molecule i, and $g_R(\sigma_i)$ is the contact radial distribution function of a LJ chain, calculated with an expression fitted to LJ simulation data (Johnson et al., 1994).

Concerning the association term (Eq. (5)), X_i^α is the fraction of molecule i not bonded at sites of type α, and M_i the number of sites of type α on molecule i. The value of X_i^α is estimated from a mass-action equation, which includes a term defining the association strength between different sites. The strength depends on two characteristic parameters, the bonding energy, $\varepsilon^{HB}_{\alpha-\beta,ii}/k_B$, and volume of association, $\kappa^{HB}_{\alpha-\beta,ii}$ of association. The cross-association energy and volume are calculated by the combining rules:

$$\kappa^{HB}_{\alpha-\beta,ij} = \left(\frac{\sqrt[3]{\kappa^{HB}_{\alpha-\beta,ii}}+\sqrt[3]{\kappa^{HB}_{\alpha-\beta,jj}}}{2}\right)^3 \tag{6}$$

$$\frac{\varepsilon^{HB}_{\alpha-\beta,ij}}{k_B} = \alpha^{HB}_{ij}\sqrt{\frac{\varepsilon^{HB}_{\alpha-\beta,ii}}{k_B}\frac{\varepsilon^{HB}_{\alpha-\beta,jj}}{k_B}} \tag{7}$$

where α_{ij}^{HB} is a correction term added to account for possible deviations of the cross-association energy from the geometric mean. The reader is referred to the original publication for further details on the equation (Blas and Vega, 1997).

In summary, five molecular parameters m, σ, ε/k_B, κ^{HB} and ε^{HB}/k_B are used to describe associating compounds. These parameters are fitted to experimental vapor pressure and saturated liquid density, although it is worth to use physical information to minimize the number of parameters to be optimized.

The surface tension of *n*-hydrofluorolefins and their blends is calculated by using the Density Gradient Theory (DGT) approach (Cahn and Hilliard, 1958) coupled into soft-SAFT. DGT provides a density functional for the local Helmholtz free energy density a of a fluid along the interface to account for the inhomogeneity of the region. This is done by expanding a in a Taylor series about $a_0(\rho)$, truncating it after the second term. The first term represents the Helmholtz energy density of a homogeneous fluid, evaluated at a local density between the bulk densities, while the second is proportional to the square of the molar density gradient. In the absence of an external potential, the expression reads:

$$A = \int \left[a_0(\rho) + \sum_i \sum_j \frac{1}{2} c_{ij} \nabla\rho_i \nabla\rho_j \right] d^3r \qquad (8)$$

where the integration is performed in the entire system volume, ρ_i is the molar density of component i, and c is the influence parameter, which is treated phenomenologically as a parameter fitted to experimental surface tension data.

Density profiles can be obtained by the DGT minimizing the total free energy of the system. Davis and Scriven (Davis and Scriven, 1982) proved that the chemical potential of a species remains constant across the interface.

Finally, the viscosity of refrigerants is evaluated by coupling the Free Volume Theory **(**FVT) (Allal et al., 2001b, 2001a) with soft-SAFT (Llovell et al., 2013b). The FVT allows the calculation of the viscosity from the use of thermodynamic variables and is expressed from the sum of two terms:

$$\eta = \eta_0 + \Delta\eta \qquad (9)$$

where η_0 is the viscosity of the dilute gas, and $\Delta\eta$ is a term used to correct the viscosity calculations for dense fluids. The dilute term is based on the modified Chapman-Enskog

theory (Chung et al., 1988). This expression includes the critical properties, acentric factor and an empirical hydrogen-bonding related parameter κ. As the contribution of κ is minimal (Llovell and Vega, 2014), the value recommended by Chung et al. for alkanols is taken here for HFOs, without further adjustements.

The dense-state term $\Delta\eta$ is based on two interconnected principles: (1) the viscosity to the microstructure of the fluid representing the molecules as spheres connected by a spring (dumbbell model), and (2) the idea that the viscosity is linked to the empty space among the molecules, following the Doolitle exponential expression (Doolittle and Peterson, 1951); this second principle gives the name to the theory. Details on the diluted and dense terms, as well as how they are related to soft-SAFT can be found in previous contributions (Cané et al., 2017; Llovell et al., 2013b, 2013a).

The FVT treatment contains three adjustable parameters, α, B and L_v, which are fitted to pure viscosity data at several pressures, as done for 1-alkanols and several families of ionic liquids in previous works (Llovell et al., 2013c, 2013a; Llovell and Vega, 2014; Pereiro et al., 2017). The proposed Spider Web parametrization (Cané et al., 2017), used to avoid parameters degeneracy, could not be followed here due to the lack of enough experimental data for mixtures of n-hydrofluorolefin mixtures.

The extension of the theory to mixtures is done by using direct compositional rules, as done in a previous contribution for HFCs (Llovell et al., 2013a).

$$\alpha_{mixt} = \sum_i x_i \alpha_i \quad (10)$$

$$B_{mixt} = \sum_i x_i B_i \quad (11)$$

$$L_{v,mixt} = \sum_i x_i L_{v,i} \quad (12)$$

3. Molecular Models

In this work, a molecular model for several HFOs is proposed in a similar manner as previously done for HFCs (Vilaseca et al., 2010). HFOs are modeled with soft-SAFT as homonuclear chains formed by m spherical segments of diameter σ with the same dispersive energy ε. In addition, the presence of fluorine atoms in their structure causes them to have a high electronegativity and, therefore, show a high dipolar moment. This effect is mimicked with the association term of the soft-SAFT equation by the addition of two associating points that have a volume κ^{HB} and an energy of association, ε^{HB}. The directional forces between

partial loads are opposed and one associating site represents the fluors (negative) and the other one the hydrogen (positive) present in the molecule.

In order to limit the number of adjustable parameters, the association volume κ^{HB}, which was set to a constant value for all HFCs, (Vilaseca et al., 2010), is transferred to HFOs, considering the similarities among these molecules. It is expected that the structural differences will be reflected in the remaining parameters. The molecular parameters have been fitted to available experimental saturated liquid density and vapor pressure, using the experimental data provided in Table 1.

4. Results

4.1. Pure HFOs

The characterization of a selection of HFOs is presented in this section. In particular, 2,3,3,3-tetrafluoroprop-1-ene (R1234yf), trans-1,3,3,3-tetrafluoroprop-1-ene (R1234ze(E)), cis-1,3,3,3-tetrafluoroprop-1-ene (1234ze(Z)), trans-1-chloro-3,3,3-trifluoroprop-1-ene (R1233zd), 3,3,3-trifluoroprop-1-ene (R1243zf) and cis-1,1,1,4,4,4-hexafluoro-2-butene (R1336mzz(Z)) have been optimized following the model proposed in section 3 and sketched in Figure S1 of the Supplementary Information; the molecular parameters for each HFO are shown in Table 1. It is interesting to remark that the m and σ parameters of the isomers R1234ze(E) and R1234ze(Z) have been kept equal, since only their atomic distribution along the molecule changes. The volume of these two molecules and R1234yf is very similar, and this is noticed by having approximately the same soft-SAFT molecular volume, estimated as the product $m\sigma^3$. This product increases with the addition of a chlorine (R1233zd, where the segment diameter σ is higher) or by the addition of more carbons (R1336mzz(Z), increasing the chain length m). In general terms, the volumetric parameters of soft-SAFT found for these compounds are similar to those obtained for the perfluoroalkanes family in a previous work (Dias et al., 2009), while the dispersive energy, ε/k_B, and association energy parameters, ε^{HB}/k_B are within the same values as those found for HFCs (Vilaseca et al., 2010).

With these parameters, the description of the phase equilibria of the studied refrigerants is very accurate as compared to the experimental data (or to correlated data from experiments for the case of R1234yf) used for the fitting, with an average absolute deviation percentage (AAD%) below 0.5% for the saturated liquid density (AAD_ρ) and 3.4% for the vapor pressure

(AAD_P), in all cases (see Table 1). The temperature-density and pressure-temperature diagrams of these compounds are depicted in Figures 1a and 1b, respectively. The Figures also include additional available data not used in the fitting, such as the saturated vapor densities (Kondou et al., 2015; Leck, 2009; Tanaka et al., 2016), near-critical region data (Tanaka and Higashi, 2010) and the critical points. The description of the vapor density is very well predicted in all cases, while the critical points are slightly overestimated, as expected from a mean-field theory such as soft-SAFT. Although this can be corrected using a crossover soft-SAFT (Llovell et al., 2004), at the expenses of more computational time, we have preserved the simpler classical soft-SAFT, provided that the region of application for refrigeration remains below the critical temperature.

The predictive capability of the model has been assessed with derivative properties data for those molecules where there is available data. In particular, the heat capacity and the speed of sound have been predicted with soft-SAFT and compared to data at different isotherms for R1234yf, in Figure 2, and R1234ze(E), in the Supplementary Information (Figure S2). The agreement between the experimental data (Lago et al., 2011; Liu et al., 2018, 2017) and the soft-SAFT predictions is very good for the heat capacity (AAD% of 2.41% and 3.71% for R1234yf and R1234ze (E), respectively) with the exception of the highest temperature and low pressure region. This is possibly related to the slight overprediction of the critical point, having an impact on the heat capacity calculation. Also, good predictions are obtained for the speed of sound (AAD% of 3.39% and 4.23% for R1234yf and R1234ze (E), respectively), with some higher deviations (around 10%) at the lowest temperature. As the speed of sound calculation depends on other derivative properties, the accumulation of minor deviations can impact the estimation of this property (Llovell and Vega, 2006). In any case, it is important to recall that the accurate prediction of second-order properties represents a challenge for any EoS, becoming a stringent test for any model.

The characterization of pure HFOs is completed by describing two additional properties of interest in the design of new refrigerants: the surface tension and the viscosity. The surface tension and the viscosity have direct impact on the heat transfer coefficient during condensation and evaporation, affecting the efficiency and capacity of air conditioning and heat pump systems (Kondou et al., 2015). In addition, high liquid viscosities also increase pressure drop resulting in in a reduction of the system capacity (Prapainop and Suen, 2012). The surface tension of the same HFOs modeled in Figure 1 is plotted in Figure 3. The

comparison between the experimental data (Kondou et al., 2015; Zhao et al., 2014) and DGT + soft-SAFT reveals an excellent agreement in the whole range of temperature in all cases, with a slight overprediction of the point where the surface tension vanishes, due to the overprediction of the critical point. The influence parameter was fitted for each HFO, showing similar values among them (see Table 2) and also with those found for HFCs in previous work (Vilaseca et al., 2010). Finally, the viscosity of R1234yf, R1234ze (E) and R1336-mzz(Z) has been evaluated using the FVT coupled with soft-SAFT in a wide range of temperature and pressure, as shown in the three-dimensional Figure 4. The lines correspond to the theory results using the FVT parameters indicated in Table 3. The parameters are temperature and pressure independent, being able to describe the fluid at different conditions with an average deviation of approximately 2%.

4.2. Binary blends

Once the pure HFOs have been adequately parametrized, the next step consists on the description of the thermodynamic behavior of binary mixtures with HFCs, as they will constitute the 4th generation blends. For this purpose, some common HFCs have been revisited in this work. Although a set of molecular parameters was available from a previous contribution (Vilaseca et al., 2010), that work was done including a renormalization group treatment for the critical region (Llovell et al., 2004) that is not included here, as there is no need for the range of conditions applied to the current work. Consequently, some minor readjustements have been done to the parameters, in order to better fit the vapor pressure of these systems. The revised molecular parameters for the HFCs are provided in Table 4. This reparametrisation affects the surface tension and viscosity parameters, which are also readjusted for R32 and shown in Table 5.

Although HFOs and HFCs have several common structures, the double bond present in the HFOs has an impact on the binary systems, preventing them from behaving as ideal mixtures. Differences in the intermolecular interactions are corrected by the inclusion of the dispersive energy binary parameter, ξ (Eq. 3), and/or the cross association binary parameter, α^{HB} (Eq. 7). This procedure is done by fitting these parameters to an isotherm set of data. Then, the parameter is used in a predictive manner for the calculation of other isotherms or isobars. Table 6 summarizes the binary parameters used for each mixture, including those cases in which pure predictions (i.e. binary parameters equal to one) were very accurate.

Figure 5 depicts the vapor-liquid (VLE) diagram of the most studied HFO, R1234yf, with the most used HFC, R32, at different temperatures in the range 273-333K. As it can be seen, excellent agreement is reached at all temperatures between the available experimental data (Akasaka, 2013) and the soft-SAFT calculations. The mixture R1234yf + R32 required the fitting of the two energetic parameters for a more accurate description, although both of them are relatively close to the unity (see Table 6). In a similar manner, an excellent description for the VLE of R1234ze(E) + R32, shown in the Supplementary Information (Figure S3), is obtained using only one binary parameter, the crossed dispersive energy (Eq. 3). It is important to remind that these parameters are temperature-independent and can be transferred to other working conditions.

Once the VLE diagram is properly described, the robustness of the model and parameters is assessed by predicting the interfacial tension and the viscosity at three different isopleths. The results are plotted in Figures 6 and 7, respectively, for the mixture with R1234yf, and Figures S4 and S5, for the mixture with R1234ze(E). In all cases, the theory reproduces the interfacial tension of the mixture with remarkable accuracy when compared to the data (Cui et al., 2016) in the whole range of temperature tested. The viscosity is also predicted in good agreement with some deviations at the lowest R32 composition. It is important to consider that the viscosity calculation is strongly affected by any minor deviation in the density and pressure according to the formulation of the FVT method. While the introduction of a binary parameter can improve the calculations, we preserve here the transferability of the approach as the overall agreement is very good and consistent.

The VLE of R1234yf with two additional HFCs, R134a and R152, is also evaluated, as their narrow VLEs and the azeotropic behavior make them good candidates to be used as refrigerants. The results plotted in Figure 8 show that an excellent agreement is achieved at all temperatures. In both cases, only one binary independent temperature parameter is required to account for deviations in the dispersive energy (Eq. 3), reproducing the azeotropic behavior of these blends in very good agreement with the experimental data (Kamiaka et al., 2013; Yang et al., 2018). Additionally, the blend with R125 (Figure S6 of the Supplementary Information) is predicted from the pure component parameters (so no fitting to binary data is necessary), perfectly reproducing the narrow VLE at different temperatures.

4.3. Ternary Blends

The study of HFOs and some blends with HFCs is here extended to ternary mixtures. From the characterization of the binary mixtures, prediction on multicomponent systems is possible using the same model and parameters, without the need to fit to experimental data. As an example, the thermodynamic diagram for the ternary blend R152a (GWP=124), R32 (GWP=675) and R1234yf (GWP=4) is plotted at 293.15 K in Figure 9. This mixture is a potential replacement for R134a (GWP=1430) or R125 (GWP=3500) in air conditioning equipment and experimental data are available (Yang et al., 2018). These data are compared with the mixture composition predictions provided by soft-SAFT at different pressures in Figure 9a. The binary systems with R1234yf were characterized in Figures 5 and 8b while the R32 + R152 binary was perfectly described using a ξ=0.985 (Supplementary Information, Figure S7) (Yang et al., 2018). All the parameters were transferred to predict the ternary system, without any fitting. Excellent agreement is found at all pressures (from 0.675 till 1.105 MPa) and for both phases (liquid and vapor), with all points overlapping the experimental measurements.

Taking advantage of the accurary of the model, a diagram of isobars for this mixture was built in a predictive manner. The equilibrium diagram is plotted in Figure 9b. With this information, accurate knowledge of the composition of this blend at any pressure is provided. These calculations can also be extrapolated to other temperatures.

4.4. Energetic evaluation of a refrigeration process with HFOs

As an application of the molecular model to refrigeration processes, we present here the study of the performance of new mixtures based on a blend of HFO and HFC at different ratios as compared with a very common 3rd generation refrigerant, R410A, an equimassic mixture between R32 and R125. The purpose is to substitute R125 (GWP=3500) by R1234yf (GWP=4), in order to lower the GWP of the blend, while keeping the desired thermodynamic properties and performance for the refrigeration process.

For this purpose, the efficiency of several refrigerants is evaluated in a vapor compression refrigeration circuit. This cycle is a practical scheme in the range of application from 250K up to 280K because of its simplicity and energy effectiveness, and is found in domestic, industrial and commercial refrigeration in general. A scheme of the cycle is displayed in Figure S8.

The process conditions set to implement the process simulations are summarized in Table 7. The saturated pressure for the corresponding mixture and system (P^{SAT}) can be found after securing the saturated liquid composition of the mixture and the evaporator's temperature. In an ideal refrigeration cycle, the enthalpy before the compressor would correspond to saturated vapor conditions (H_1^V) but, as the cycle being modelled pretends to simulate a real process, overheating is introduced to ensure a fully vapor phase after the evaporator. As the expansion valve is isoenthalpic, the enthalpy of the two-phases mixture at non saturated conditions after the valve (H_4^{L+V}) is automatically determined by the saturated liquid before the expansion (H_3^L). Likewise, pressures in the positions after and before the evaporator are static at 0.7MPa to compare the effect of the evaporator's temperature at the same conditions for the different mixtures being considered.

The evaluation of the efficiency is based on the calculation of the coefficient of performance (CoP), defined in Eq. (13) as a function of the specific enthalpies and the nomenclature used in Figure S9.

$$CoP = \frac{\sum q_{in}}{\sum W_{net,in}} = \frac{H_1^V - H_4^{L-V}}{H_2^V - H_1^V} = \frac{H_1^V - H_3^L}{H_2^V - H_1^V} \quad (13)$$

where points 1 and 2 correspond to the fluid before and after the compressor, and points 3 and 4 are before and after the expansion valve, respectively. All enthalpies are predicted with soft-SAFT using the models established in previous sections.

Firstly, a study of the effect of the proportion HFO/HFC within the mixture is carried out at a fixed evaporator's temperature of T=265K (standard working refrigeration temperature). As it can be seen in Figure 10a, the increase of HFOs composition diminishes the CoP of the system. The CoP of several commercial HFO-based mixtures (R454A, R454B, R454C and R457A) has also been added to the diagram for comparison. Among them, R454B gets the major efficiency, as it has the highest HFC composition. The studied R1234yf + R32 + R152a ternary blend becomes more competitive at higher HFO composition, even if the CoP decreases, as it happens in all mixtures. Considering both CoP and GWP factors, the best 4th generation refrigerant mixture to replace R410A is R32+R1234yf (3:1).

Based on these results, an HFO composition of 0.25 has been fixed and the effect of the evaporator temperature on the CoP has been studied for several blends, maintaining this HFO ratio. The results are displayed in Figure 10b, including R410 for comparison. In all

cases, the CoP rises with an increase of the evaporator temperature. This is a natural consequence of the increase of the vapor enthalpy after the evaporator. It is also observed that R32 provides a higher CoP than R125, which is good as this later compound has a higher GWP. Again, the R32 + R1234yf (3:1) mixture offers the best performance among the alternatives to replace R410A, even if none of them reaches the CoPs of R410A in the studied temperature range. In this regard, a compromise between efficiency and a low GWP must be achieved and a deeper energy analysis is required to fully assess the R32 + R1234yf (3:1) mixture for this application, which is out of the scope of the current manuscript, mainly focused on the thermodynamic models.

5. Conclusions

In this contribution, the molecular-based EoS soft-SAFT have been used, combined with other molecular theories for interfacial and viscosity calculations to study the behavior of thermodynamic, interfacial and transport properties of HFOs compounds relevant for the refrigeration industry. A physically meaningful set of molecular parameters were proposed for each compound of the family able to capture the main physical features of HFOs and accurately describing the saturated densities and vapor pressures of these compounds. The model was validated for R1234yf and R1234ze(E), the two most commonly used HFOs, predicting their heat capacity and speed of sound with accuracy. The model also accurately described surface tension and the viscosity of these compounds.

The VLE of selected binary blends of these HFOs in combination with an HFC was described using one binary temperature independent energy parameter, except for one mixture where two fitted parameters gave a better estimation. The agreement between calculations and available experimental data for ideal and azeotropic mixtures was excellent in all cases. Furthermore, the model provided accurate predictions of the interfacial tension and viscosity of some of these blends. Finally, a ternary mixture was predicted in good agreement with the data, using all the data transferred from the binary systems. This highlights the transferability of the model to address multicomponent systems for which experimental data may not be available. The study was completed with several process simulations of a vapor compression refrigeration circuit, where several fourth generation mixtures were compared with the third generation R410A HFCs blend. Overall, the best performance was obtained with R32+R1234yf (3:1), although the CoP slightly decreased

compared to R410A. However, this is largely compensated by a considerable reduction of the GWP of the system.

Acknowledgements

GESPA has been recognized as Consolidated Research Group by the Catalan government (2017-SGR-1016). This research is supported by Project KET4F-Gas – SOE2/P1/P0823, which is co-financed by the European Regional Development Fund within the framework of Interreg Sudoe Programme. Additional funding has been provided by Khalifa University of Science and Technology, project CIRA2018-121.

Bibliography

Akasaka, R., 2013. Thermodynamic property models for the difluoromethane (R-32)+trans-1,3,3,3-tetrafluoropropene (R-1234ze(E)) and difluoromethane+2,3,3,3-tetrafluoropropene (R-1234yf) mixtures. Fluid Phase Equilib. 358, 98–104. https://doi.org/10.1016/j.fluid.2013.07.057

Al Ghafri, S.Z., Rowland, D., Akhfash, M., Arami-Niya, A., Khamphasith, M., Xiao, X., Tsuji, T., Tanaka, Y., Seiki, Y., May, E.F., Hughes, T.J., 2019. Thermodynamic properties of hydrofluoroolefin (R1234yf and R1234ze(E)) refrigerant mixtures: Density, vapour-liquid equilibrium, and heat capacity data and modelling. Int. J. Refrig. 98, 249–260. https://doi.org/10.1016/j.ijrefrig.2018.10.027

Alam, J., Miyara, A., Kariya, K., Kontomaris, K.K., 2018. 1336mzz (Z)) by Tandem Capillary Tubes Method. https://doi.org/10.1021/acs.jced.8b00036

Allal, A., Boned, C., Baylaucq, A., 2001a. Free-volume viscosity model for fluids in the dense and gaseous states. Phys. Rev. E 64, 011203. https://doi.org/10.1103/PhysRevE.64.011203

Allal, A., Moha-Ouchane, M., Boned, C., 2001b. A New Free Volume Model for Dynamic Viscosity and Density of Dense Fluids Versus Pressure and Temperature. Phys. Chem. Liq. 39, 1–30. https://doi.org/10.1080/00319100108030323

Blas, F.J., Vega, L.F., 1998. Prediction of Binary and Ternary Diagrams Using the Statistical Associating Fluid Theory (SAFT) Equation of State. Ind. Eng. Chem. Res. 37, 660–674. https://doi.org/10.1021/ie970449+

Blas, F.J., Vega, L.F., 1997. Thermodynamic behaviour of homonuclear and heteronuclear Lennard-Jones chains with association sites from simulation and theory. Mol. Phys. 92, 135–150. https://doi.org/10.1080/002689797170707

Cahn, J.W., Hilliard, J.E., 1958. Free Energy of a Nonuniform System .1. Interfacial Free Energy. J. Chem. Phys. 28, 258–267. https://doi.org/10.1063/1.1744102

Cané, E., Llovell, F., Vega, L.F., 2017. Accurate viscosity predictions of linear polymers from n-alkanes data. J. Mol. Liq. 243. https://doi.org/10.1016/j.molliq.2017.08.033

Chapman, W.G., Gubbins, K.E., Jackson, G., Radosz, M., 1990. New reference equation of state for associating liquids. Ind. Eng. Chem. Res. 29, 1709–1721. https://doi.org/10.1021/ie00104a021

Chung, T.H., Ajlan, M., Lee, L.L., Starling, K.E., 1988. Generalized Multiparameter Correlation for Nonpolar and Polar Fluid Transport Properties. Ind. Eng. Chem. Res. 27, 671–679. https://doi.org/10.1021/ie00076a024

Cui, J., Bi, S., Meng, X., Wu, J., 2016. Surface Tension and Liquid Viscosity of R32+R1234yf and R32+R1234ze. J. Chem. Eng. Data 61, 950–957. https://doi.org/10.1021/acs.jced.5b00798

Davis, H.T., Scriven, L.E., 1982. Stress and structure in fluid phase interfaces. Adv. Chem. Phys. 49, 357. https://doi.org/10.1002/9780470142691.ch6

Dias, A.M.A., Llovell, F., Coutinho, J.A.P., Marrucho, I.M., Vega, L.F., 2009. Thermodynamic characterization of pure perfluoroalkanes, including interfacial and second order derivative properties, using the crossover soft-SAFT EoS. Fluid Phase Equilib. 286. https://doi.org/10.1016/j.fluid.2009.08.018

Dias, A.M.A., Pàmies, J.C., Coutinho, J.A.P., Marrucho, I.M., Vega, L.F., 2004. SAFT Modeling of the Solubility of Gases in Perfluoroalkanes. J. Phys. Chem. B 108, 1450–1457. https://doi.org/10.1021/jp036225o

Doolittle, A.K., Peterson, R.H., 1951. Preparation and Physical Properties of a Series of n-Alkanes. J. Am. Chem. Soc. 73, 2145–2151. https://doi.org/10.1021/ja01149a069

Ferreira, M.L., Araújo, J.M.M., Pereiro, A.B., Vega, L.F., 2019. Insights into the influence of the molecular structures of fluorinated ionic liquids on their thermophysical properties. A soft-SAFT based approach. Phys. Chem. Chem. Phys. https://doi.org/10.1039/c8cp07522k

Fouad, W.A., Vega, L.F., 2018a. Next generation of low global warming potential refrigerants: Thermodynamic properties molecular modeling. AIChE J. 63, 250–262. https://doi.org/10.1002/aic.15859

Fouad, W.A., Vega, L.F., 2018b. Transport properties of HFC and HFO based refrigerants using an excess entropy scaling approach. J. Supercrit. Fluids 131, 106–116. https://doi.org/10.1016/j.supflu.2017.09.006

Goetzler, W., Sutherland, T., Rassi, M., Burgos, J., 2014. Research & Development Roadmap for Next-Generation Low Global Warming Potential Refrigerants. DOE Off. Energy Effic. Renew. Energy 1–60.

He, M., Qi, X., Liu, X., Su, C., Lv, N., 2015. Estimating the viscosity of pure refrigerants and their mixtures by free-volume theory. Int. J. Refrig. https://doi.org/10.1016/j.ijrefrig.2015.03.010

Heath, E.A., 2017. Amendment to the Montreal Protocol on Substances that Deplete the Ozone Layer (Kigali Amendment). Int. Leg. Mater. 56, 193–205. https://doi.org/10.1017/ilm.2016.2

Johnson, J.K., Müller, E.A., Gubbins, K.E., 1994. Equation of State for Lennard-Jones Chains. J. Phys. Chem. 98, 6413–6419. https://doi.org/10.1021/j100076a028

Johnson, J.K., Zollweg, J.A., Gubbins, K.E., 1993. The Lennard-Jones equation of state revisited. Mol. Phys. 78, 591–618. https://doi.org/10.1080/00268979300100411

Kamiaka, T., Dang, C., Hihara, E., 2013. Vapor-liquid equilibrium measurements for binary mixtures of R1234yf with R32, R125, and R134a. Int. J. Refrig. 36, 965–971. https://doi.org/10.1016/j.ijrefrig.2012.08.016

Kang, K., Wang, X., Kontogeorgis, G.M., Liang, X., 2018. Modeling Hydrofluoroolefins with the Cubic Plus Association and Perturbed-Chain Statistical Associating Fluid Theory Equations of State. Ind. Eng. Chem. Res. 57, 17289–17300. https://doi.org/10.1021/acs.iecr.8b04813

Kondou, C., Nagata, R., Nii, N., Koyama, S., Higashi, Y., 2015. Surface tension of low GWP refrigerants R1243zf, R1234ze(Z), and R1233zd(E). Int. J. Refrig. 53, 80–89. https://doi.org/10.1016/j.ijrefrig.2015.01.005

Lago, S., Albo, P.A.G., Brignolo, S., 2011. Speed of sound results in 2,3,3,3-tetrafluoropropene (R-1234yf) and trans -1,3,3,3-tetrafluoropropene (R-1234ze(E)) in the temperature range of (260 to 360) K. J. Chem. Eng. Data 56, 161–163. https://doi.org/10.1021/je100896n

Leck, T., 2009. Evaluation of HFO-1234yf as a Potential Replacement for R-134a in Refrigeration Applications. Proc. 3rd IIR Conf. Thermophys. Prop. … 155, 1–9.

Li, Y., Fouad, W.A., Vega, L.F., 2019. Interfacial anomaly in low global warming potential refrigerant blends as predicted by molecular dynamics simulations. Phys. Chem. Chem. Phys. 21, 22092–22102. https://doi.org/10.1039/c9cp03231b

Liu, Y., Zhao, X., He, H., Wang, R., 2018. Heat Capacity of R1234ze(E) at Temperatures from 313 to 393 K and Pressures up to 10 MPa. J. Chem. Eng. Data 63, 113–118. https://doi.org/10.1021/acs.jced.7b00713

Liu, Y., Zhao, X., Lv, S., He, H., 2017. Isobaric Heat Capacity Measurements for R1234yf from 303 to 373 K and Pressures up to 12 MPa. J. Chem. Eng. Data 62, 1119–1124. https://doi.org/10.1021/acs.jced.6b00959

Lloret, J.O., Vega, L.F., Llovell, F., 2017. Accurate description of thermophysical properties of Tetraalkylammonium Chloride Deep Eutectic Solvents with the soft-SAFT equation of state. Fluid Phase Equilib. 448, 81–93. https://doi.org/10.1016/j.fluid.2017.04.013

Llovell, F., Marcos, R.M., Vega, L.F., 2013a. Transport properties of mixtures by the soft-SAFT + Free-volume theory: Application to mixtures of n-alkanes and hydrofluorocarbons. J. Phys. Chem. B 117. https://doi.org/10.1021/jp401754r

Llovell, F., Marcos, R.M., Vega, L.F., 2013b. Free-volume theory coupled with soft-SAFT for viscosity calculations: Comparison with molecular simulation and experimental data. J. Phys. Chem. B 117. https://doi.org/10.1021/jp401307t

Llovell, F., Oliveira, M.B., Coutinho, J.A.P., Vega, L.F., 2015. Solubility of greenhouse and acid gases on the [C_4mim][$MeSO_4$] ionic liquid for gas separation and CO_2

conversion. Catal. Today 255, 87–96. https://doi.org/10.1016/j.cattod.2014.12.049

Llovell, F., Pàmies, J.C., Vega, L.F., 2004. Thermodynamic properties of Lennard-Jones chain molecules: Renormalization-group corrections to a modified statistical associating fluid theory. J. Chem. Phys. 121, 10715–10724. https://doi.org/10.1063/1.1809112

Llovell, F., Valente, E., Vilaseca, O., Vega, L.F., 2011. Modeling complex associating mixtures with [$C_n$mim][Tf_2N] ionic liquids: Predictions from the soft-SAFT equation. J. Phys. Chem. B 115, 4387–4398. https://doi.org/10.1021/jp112315b

Llovell, F., Vega, L.F., 2014. Assessing ionic liquids experimental data using molecular modeling: [Cnmim][BF4] case study. J. Chem. Eng. Data 59, 3220–3231. https://doi.org/10.1021/je5002472

Llovell, F., Vega, L.F., 2006. Prediction of thermodynamic derivative properties of pure fluids through the soft-SAFT equation of state. J. Phys. Chem. B 110. https://doi.org/10.1021/jp0608022

Llovell, F., Vilaseca, O., Jung, N., Vega, L.F., 2013c. Water+1-alkanol systems: Modeling the phase, interface and viscosity properties. Fluid Phase Equilib. 360, 367–378. https://doi.org/10.1016/j.fluid.2013.10.002

McLinden, M.O., Brown, J.S., Brignoli, R., Kazakov, A.F., Domanski, P.A., 2017. Limited options for low-global-warming-potential refrigerants. Nat. Commun. https://doi.org/10.1038/ncomms14476

McLinden, M.O., Kazakov, A.F., Steven Brown, J., Domanski, P.A., 2014. A thermodynamic analysis of refrigerants: Possibilities and tradeoffs for Low-GWP refrigerants. Int. J. Refrig. https://doi.org/10.1016/j.ijrefrig.2013.09.032

Meng, X., Qiu, G., Wu, J., Abdulagatov, I.M., 2013. Viscosity measurements for 2,3,3,3-tetrafluoroprop-1-ene (R1234yf) and trans-1,3,3,3-tetrafluoropropene (R1234ze(E)). J. Chem. Thermodyn. 63, 24–30. https://doi.org/10.1016/j.jct.2013.03.013

Mondéjar, M.E., McLinden, M.O., Lemmon, E.W., 2015. Thermodynamic Properties of trans -1-Chloro-3,3,3-trifluoropropene (R1233zd(E)): Vapor Pressure, (p , ρ, T) Behavior, and Speed of Sound Measurements, and Equation of State. J. Chem. Eng. Data 60, 2477–2489. https://doi.org/10.1021/acs.jced.5b00348

Mota-Babiloni, A., Makhnatch, P., Khodabandeh, R., 2017. Recent investigations in HFCs substitution with lower GWP synthetic alternatives: Focus on energetic performance and environmental impact. Int. J. Refrig. https://doi.org/10.1016/j.ijrefrig.2017.06.026

Pàmies, J.C., Vega, L.F., 2001. Vapor−Liquid Equilibria and Critical Behavior of Heavy n -Alkanes Using Transferable Parameters from the Soft-SAFT Equation of State. Ind. Eng. Chem. Res. 40, 2532–2543. https://doi.org/10.1021/ie000944x

Pedrosa, N., Vega, L.F., Coutinho, J.A.P., Marrucho, I.M., 2006. Phase Equilibria Calculations of Polyethylene Solutions from SAFT-Type Equations of State. Macromolecules 39, 4240–4246. https://doi.org/10.1021/ma060584a

Pereiro, A.B., Llovell, F., Araújo, J.M.M., Santos, A.S.S., Rebelo, L.P.N., Piñeiro, M.M., Vega, L.F., 2017. Thermophysical Characterization of Ionic Liquids Based on the

Perfluorobutanesulfonate Anion: Experimental and Soft-SAFT Modeling Results. ChemPhysChem 18, 2012–2023. https://doi.org/10.1002/cphc.201700327

Prapainop, R., Suen, K.O., 2012. Effects of refrigerant properties on refrigerant performance comparison: A review. Int. J. Eng. Res. Appl. 2, 486–493.

Raabe, G., 2019. Molecular simulation studies on refrigerants past – present – future. Fluid Phase Equilib. 485, 190–198. https://doi.org/10.1016/j.fluid.2018.12.022

Raabe, G., 2017. Applications of Molecular Simulations to Studies on Working Fluids, in: Molecular Simulation Studies on Thermophysical Properties. Springer, pp. 257–289.

Raabe, G., 2016. Molecular simulation studies in hydrofluoroolefine (HFO) working fluids and their blends. Sci. Technol. Built Environ. 22, 1077–1089. https://doi.org/10.1080/23744731.2016.1206796

Raabe, G., 2015. Molecular Simulation Studies on the Vapor–Liquid Equilibria of the *cis* - and *trans* -HCFO-1233zd and the *cis* - and *trans* -HFO-1336mzz. J. Chem. Eng. Data 60, 2412–2419. https://doi.org/10.1021/acs.jced.5b00286

Raabe, G., 2013. Molecular Simulation Studies on the Vapor–Liquid Phase Equilibria of Binary Mixtures of R-1234yf and R-1234ze(E) with R-32 and CO 2. J. Chem. Eng. Data 58, 1867–1873. https://doi.org/10.1021/je4002619

Raabe, G., Maginn, E.J., 2010. A force field for 3,3,3-fluoro-1-propenes, including HFO-1234yf. J. Phys. Chem. B 114, 10133–10142. https://doi.org/10.1021/jp102534z

Schulz, M., Kourkoulas, D., 2014. Regulation (EU) No 517/2014 of the European Parliament and of the Council of 16 April 2014 on fluorinated greenhouse gases and repealing Regulation (EC) No 842/2006. Off. J. Eur. Union 2014, L150/195-230. https://doi.org/https://doi.org/10.4271/1999-01-0874

Tanaka, K., 2016. Measurements of Vapor Pressure and Saturated Liquid Density for HFO-1234ze(E) and HFO-1234ze(Z). J. Chem. Eng. Data 61, 1645–1648. https://doi.org/10.1021/acs.jced.5b01039

Tanaka, K., Akasaka, R., Sakaue, E., Ishikawa, J., Kontomaris, K.K., 2016. Thermodynamic properties of cis-1,1,1,4,4,4-hexafluoro-2-butene (HFO-1336mzz(Z)): Measurements of the pρT property and determinations of vapor pressures, saturated liquid and vapor densities, and critical parameters. J. Chem. Eng. Data 61, 2467–2473. https://doi.org/10.1021/acs.jced.6b00169

Tanaka, K., Higashi, Y., 2010. Thermodynamic properties of HFO-1234yf (2,3,3,3-tetrafluoropropene). Int. J. Refrig. 33, 474–479. https://doi.org/10.1016/j.ijrefrig.2009.10.003

Vega, L.F., Llovell, F., 2016. Review and new insights into the application of molecular-based equations of state to water and aqueous solutions. Fluid Phase Equilib. 416, 150–173. https://doi.org/10.1016/j.fluid.2016.01.024

Vega, L.F., Llovell, F., Torné, J., Freitas, S.V.D., Oliveira, M.B., Coutinho, J.A.P., 2017. Modeling Biodiesel Production and Purification – Towards a Predictive Tool, Computer Aided Chemical Engineering. https://doi.org/10.1016/B978-0-444-63965-3.50482-7

Vilaseca, O., Llovell, F., Yustos, J., Marcos, R.M., Vega, L.F., 2010. Phase equilibria, surface tensions and heat capacities of hydrofluorocarbons and their mixtures including the critical region. J. Supercrit. Fluids 55, 755–768. https://doi.org/10.1016/j.supflu.2010.10.015

Yang, T., Hu, X., Meng, X., Wu, J., 2018. Vapor–Liquid Equilibria for the Binary and Ternary Systems of Difluoromethane (R32), 1,1-Difluoroethane (R152a), and 2,3,3,3-Tetrafluoroprop-1-ene (R1234yf). J. Chem. Eng. Data 63, 771–780. https://doi.org/10.1021/acs.jced.7b00950

Zhao, G., Bi, S., Fröba, A.P., Wu, J., 2014. Liquid viscosity and surface tension of R1234yf and R1234ze under saturation conditions by surface light scattering. J. Chem. Eng. Data 59, 1366–1371. https://doi.org/10.1021/je5001457

Table Caption

Table 1. Optimized soft-SAFT parameters for the selected HFOs.

R	*m*	σ [Å]	ε/k_B [K]	ε^{HB}/k_B [K]	AAD_P [%]	AAD_ρ [%]	*Ref. (* indicates not used for fitting)*
1234yf	1.136	4.808	173.4	1909	1.870	0.438	(Leck, 2009), (Tanaka and Higashi, 2010)*
1234ze(E)	1.079	4.891	186.5	1990	1.090	0.136	(Tanaka, 2016)
1234ze(Z)	1.079	4.891	189.5	2345	0.467	0.302	(Tanaka, 2016), (Kondou et al., 2015)*
1233zd(E)	1.100	5.064	203.5	2376	1.323	0.412	(Mondéjar et al., 2015), (Kondou et al., 2015)*
1243zf	1.200	4.650	173.8	1954	0.975	0.247	(Kondou et al., 2015)
1336mzz(Z)	1.558	4.618	182.0	2446	1.560	0.872	(Tanaka et al., 2016)

Note: The volume of association, κ^{HB}, was fixed to a value of 24050 Å^3 for all hydrofluroolefins, following the same approach done for hydrofluorocarbons (Vilaseca et al., 2010).

Table 2. Optimized influence parameters for surface tension calculations of selected HFOs.

R	$c \cdot 10^{19}$ [J·m^5·mol^{-2}]	*AAD* γ [%]	*Ref.*
1234yf	1.721	1.796	(Zhao et al., 2014)
1234ze(E)	1.891	1.232	(Zhao et al., 2014)
1234ze(Z)	2.466	0.688	(Kondou et al., 2015)
1233zd(E)	3.301	1.594	(Kondou et al., 2015)
1243zf	1.699	1.901	(Kondou et al., 2015)

Table 3. Optimized viscosity parameters of selected HFOs.

R	α [J·m^3/mol·kg]	$B \cdot 10^2$	L_v [Å]	*AAD* η [%]	*Ref*
1234yf	51.15	0.3492	0.4876	1.840	(Meng et al., 2013)
1234ze(E)	45.91	0.6148	0.4876	2.200	(Meng et al., 2013)
1336mzz(Z)	68.96	0.3131	0.4454	0.907	(Alam et al., 2018)

Table 4. Soft-SAFT molecular parameters of HFCs used in 4th generation blends considered in this work.

R	m	σ [Å]	ε/k_B [K]	ε^{HB}/k_B [K]	*AAD P* [%]	*AAD* ρ [%]
32	1.321	3.529	144.40	1708	1.517	0.218
125	1.392	4.242	148.80	1685	3.480	1.130
134a	1.392	4.166	166.58	1862	0.806	0.050
152a	1.392	4.007	170.90	1885	0.646	0.034

Note: The volume of association, κ^{HB}, was fixed to a value of 24050 Å^3 for all HFCs, as done in a previous work (Vilaseca et al., 2010).

Table 5. Influence and viscosity parameters of R32 for surface tension and viscosity calculations.

R	Surface Tension	Viscosity			*Ref*
	$c \cdot 10^{19}$ [J·m^5·mol^{-2}]	α [J·m^3/mol·kg]	$B \cdot 10^2$	L_v [Å]	
32	0.580	34.60	0.7194	0.4078	(Llovell et al., 2013a; Vilaseca et al., 2010)

Table 6. Binary parameters for the dispersive (ξ) and association (α^{HB}) energies for different blends of HFOs based refrigerants. A value of 1 means that the combining rule is used, and the binary parameter has not been fitted.

Blend	ξ	α^{HB}	*Ref*
R1234yf + R32	0.960	0.9491	(Akasaka, 2013)
R1234ze(E) + R32	1.000	0.955	(Akasaka, 2013)
R1234yf + R125	1.000	1.000	(Kamiaka et al., 2013)
R1234yf + R134a	0.960	1.000	(Kamiaka et al., 2013)
R1234yf + R152a	0.950	1.000	(Yang et al., 2018)
R32 + R152a	0.985	1.000	(Yang et al., 2018)

Table 7. Design variables of the refrigeration vapor compression system simulation

Operating Point	**1**	**2**	**3**	**4**
Temperature / K	265	340	303	265
Pressure / MPa	0.7	P^{SAT}	P^{SAT}	0.7
Degrees of freedom	3 (1 Phase)	3 (1 Phase)	2 (2 Phases)	2 (2 Phases)
Fixed variables	P_1, y_{HFO}, T_1	P_2, y_{HFO}, T_2	x_{HFO}, T_3	P_1, T_1

Figures Caption

Figure 1. Phase behavior of R1234yf (blue circles), R1234ze(E) (red diamonds), R1234ze(Z) (green squares), R1233zd(E) (light blue triangles), R1243zf (magenta asterisks) and R1336mzz(Z) (black crosses). **a)** Vapor and liquid density vs. temperature, and **b)** vapor pressure in logarithmic scale vs. the reciprocal of temperature. Symbols represent the experimental or correlated data (see Table 1), while the lines correspond to the soft-SAFT modeling.

Figure 2. Second-order derivative properties of R1234yf. **a)** Heat capacity at 303K (blue circles), 323K (red diamonds), 343K (green squares) and 363K (light blue triangles). Symbols represent the experimental data (Liu et al., 2017), while the lines correspond to the soft-SAFT modeling. **b)** Speed of sound at 285K (blue circles), 310K (red diamonds), 335K (green squares) and 360K (light blue triangles). Symbols represent the experimental data (Lago et al., 2011) while the lines correspond to the soft-SAFT predictions.

Figure 3. Vapor–liquid interfacial tension for R1234yf (blue circles), R1234ze(E) (red diamonds), R1234ze(Z) (green squares), R1233zd(E) (light blue triangles) and R1243zf (black asterisks). Symbols represent the experimental data (see Table 2), while the lines correspond to the soft-SAFT +DGT modeling.

Figure 4. Three-dimensional Viscosity-Temperature-Pressure diagram for R1234yf (blue circle), R1234ze(E) (red diamond) and R1336mzz(Z) (green square) at 1 MPa, 3MPa, 5MPa and 10MPa for R1234yf and R1234ze(E) and 1MPa, 2MPa, 3MPa and 4MPa for R1336mzz(Z). Symbols represent the experimental data (see Table 3), while the lines correspond to the soft-SAFT +DGT modeling.

Figure 5: Pressure-composition diagram of the 4th generation blend R32 (1) + R1234yf (2) at 273.1K (blue circle), 283.1K (red diamond), 293.1K (green square), 303.1K (light blue triangle), 313.1K (magenta asterisk), 323.1K (black cross) and 333.1K (dark yellow plus sign). Symbols are experimental data (see Table 6) and lines are soft-SAFT calculations.

Figure 6: Surface tension as a function of temperature of the 4th generation blend R32 (1) + R1234yf (2) at molar compositions x_1=0.5193 (blue, cicle), x_1=0.6988 (red, diamond) and x_1=0.7945 (green, square). Symbols are experimental data (Cui et al., 2016) and lines are soft-SAFT predictions.

Figure 7: Viscosity as a function of temperature of the 4th generation blend R32 (1) + R1234yf (2) at molar compositions x_1=0.5193 (blue, cicle), x_1=0.6988 (red, diamond) and

x_1=0.7945 (green, square). Symbols are experimental data (Cui et al., 2016) and lines are soft-SAFT predictions.

Figure 8: Pressure-composition diagram at 273.1K (blue, circle), 283.1K (red, diamonds), 293.1K (green squares), 303.1K (light blue triangles), 313.1K (magenta asterisks), 323.1K (black crossess) and 333.1K (dark yellow plus signs) of the 4th generation blends form by a mixture of R1234yf and **a)** R134a **b)** R152a. Symbols are experimental data (Kamiaka et al., 2013; Yang et al., 2018) and lines are soft-SAFT calculations.

Figure 9: Ternary diagram of the 4th generation mixture R1234yf, R152a and R32 at 293.1K and 0.6743MPa (red), 0.7136MPa (green), 0.7891MPa (magenta), 0.8840MPa (yellow), 1.0344MPa (black), 1.1058MPa (blue). **a)** Experimental liquid phase (cross) and vapor phase (asterisks) data (Yang et al., 2018), soft-SAFT liquid phase (circles) and vapor phase (squares) predictions **b)** soft-SAFT liquid phase (continuous line) and vapor phase (dotted line) predictions.

Figure 10: Comparison of the coefficient of performance (CoP) between the 3rd generation refrigerant (R410A) (blue cross) and three alternative 4th generation refrigerants, R32 + R1234yf (red), R32 + R1234ze(E) (green), R125 + R1234yf (light blue) and R32 + R152a + R1234yf (1.5:1.5:1) (magenta) in a vapor compression refrigeration circuit. **a)** CoP as a function of the HFO composition. Symbols are additional commercial HFO-based refrigerants, such as R454A (circle), R454B (diamond), R454C (square) and R457A (triangle) **b)** CoP as a function of the evaporator's temperature, where all blends have a fixed HFO composition of 0.25, with the exception of R410.

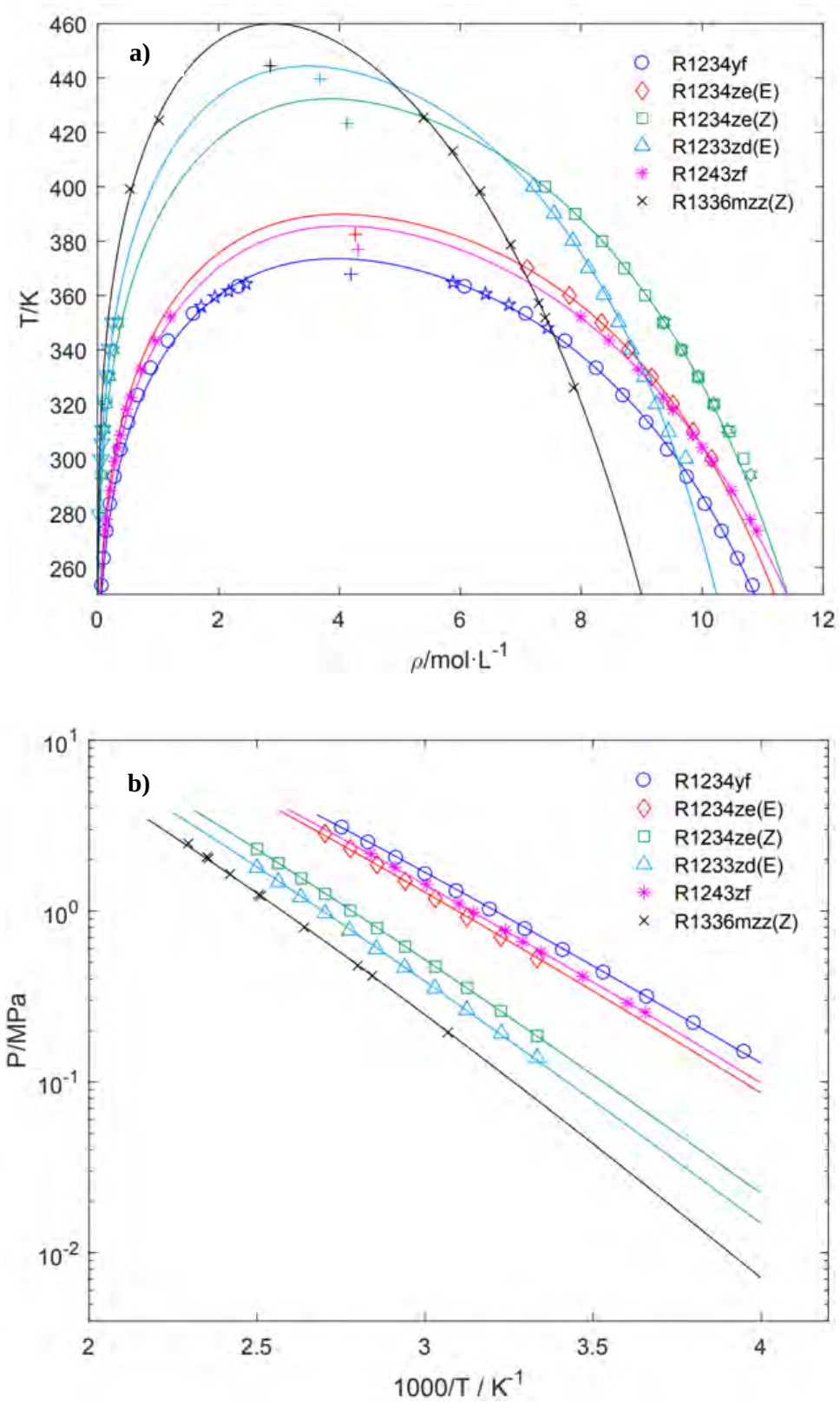

Figure 1: Albà et al.

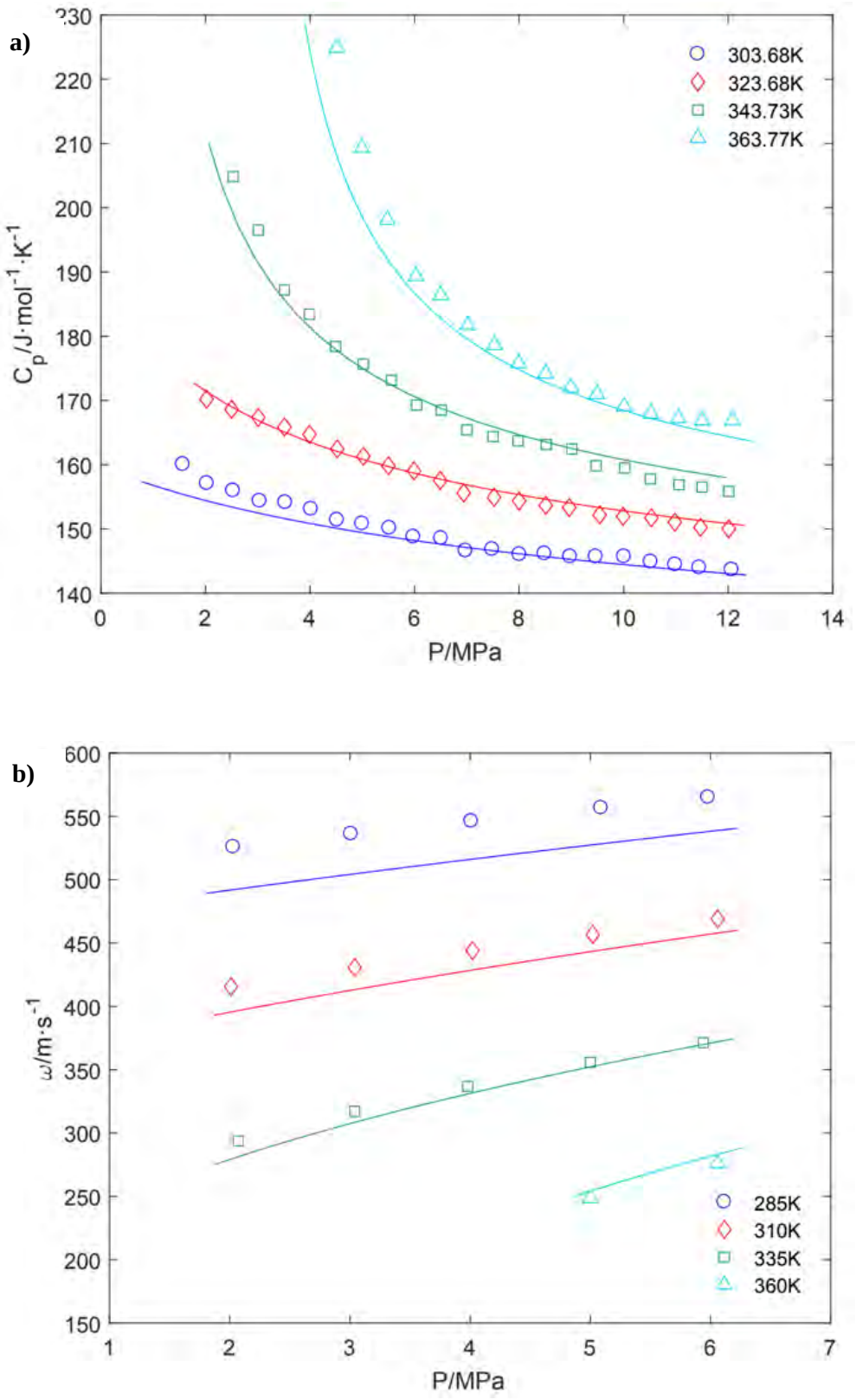

Figure 2: Albà et al.

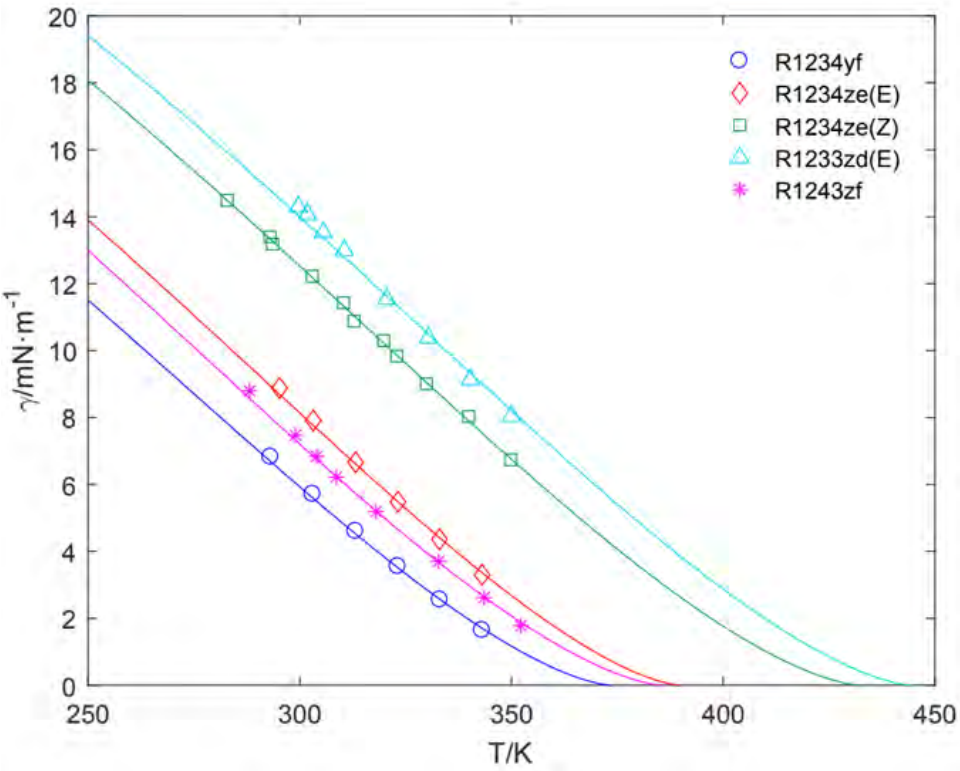

Figure 3: Albà et al.

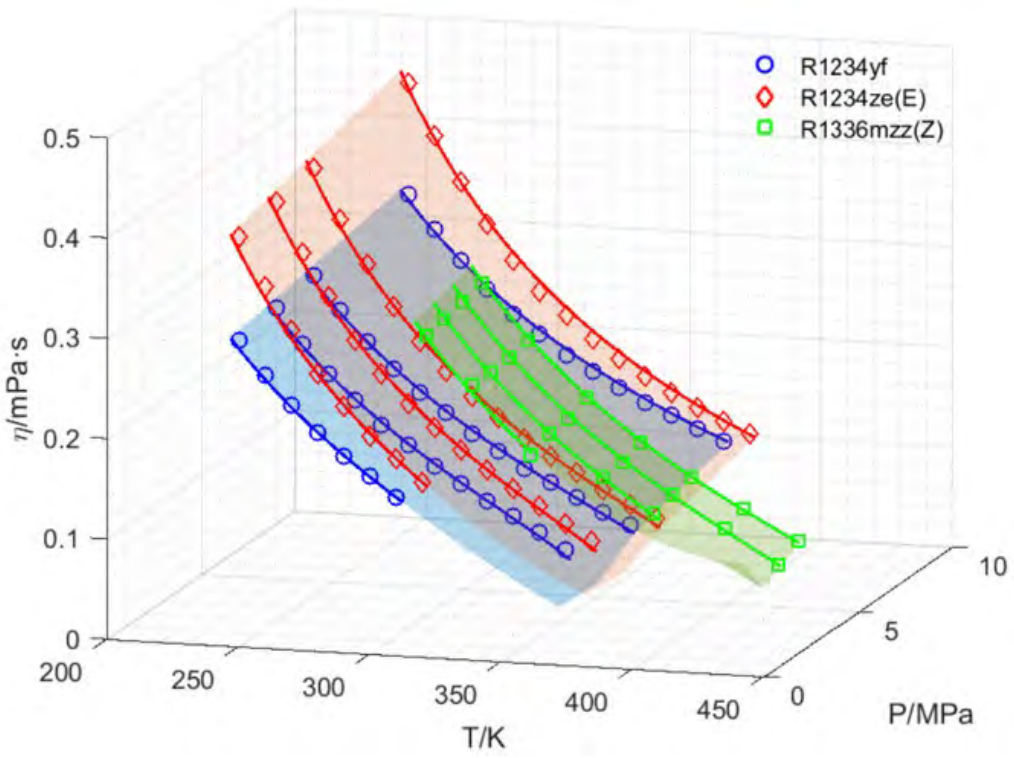

Figure 4: Albà et al.

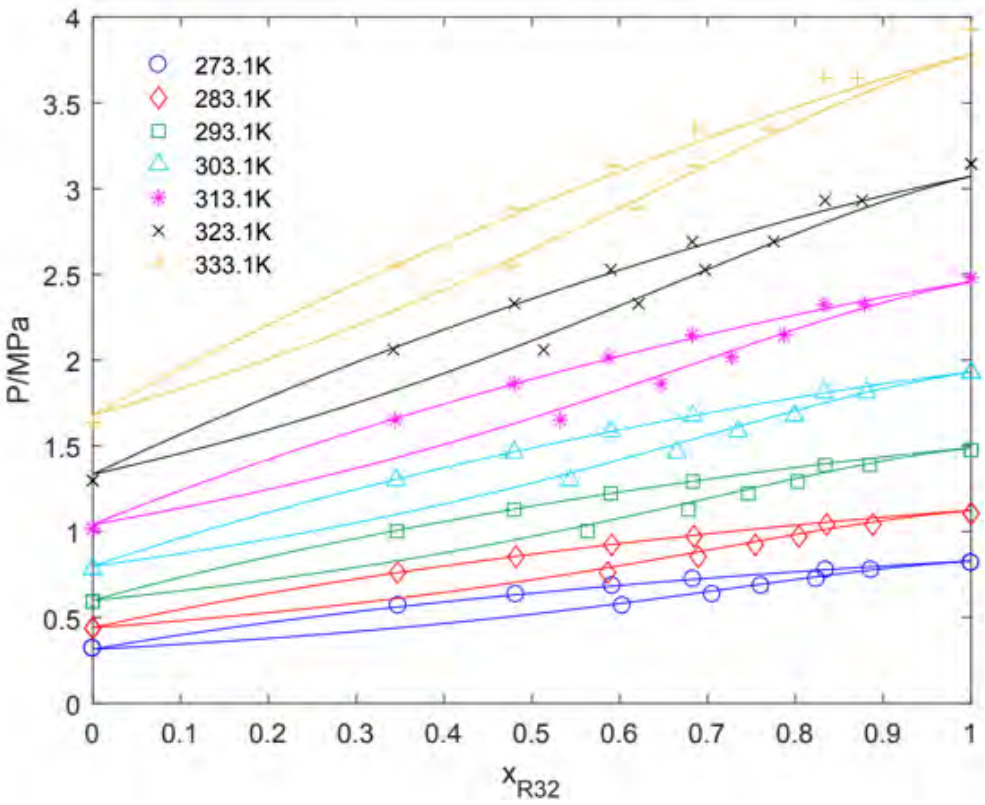

Figure 5: Albà et al.

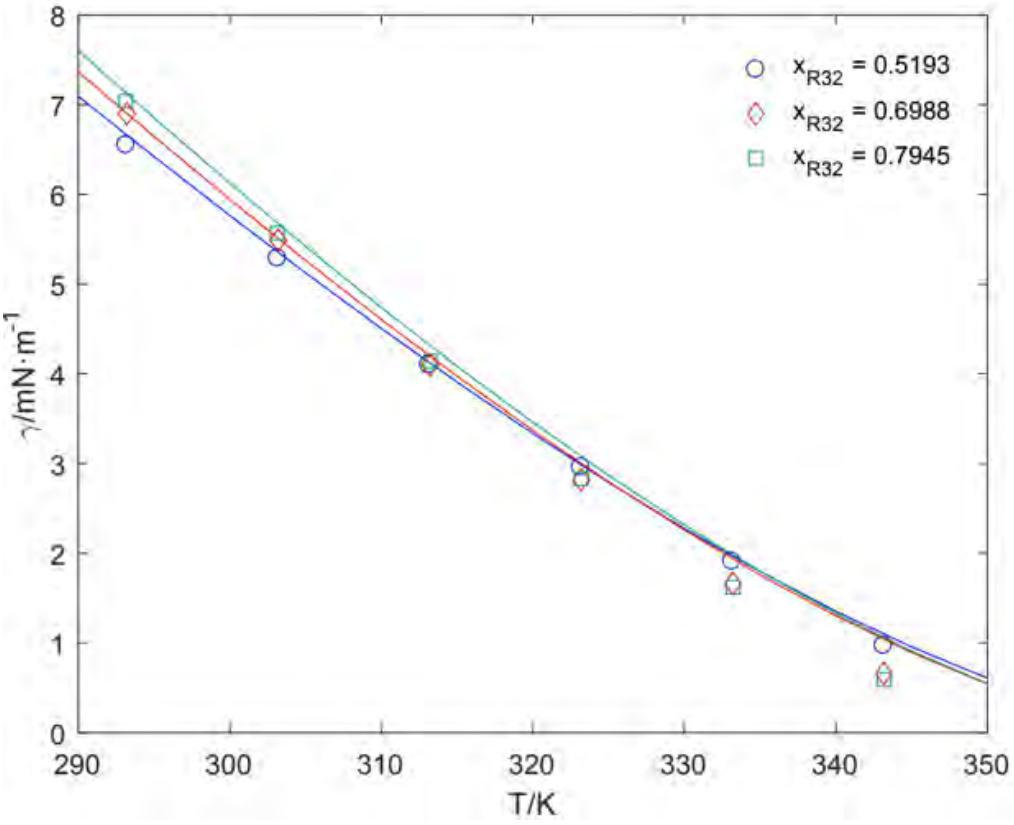

Figure 6: Albà et al.

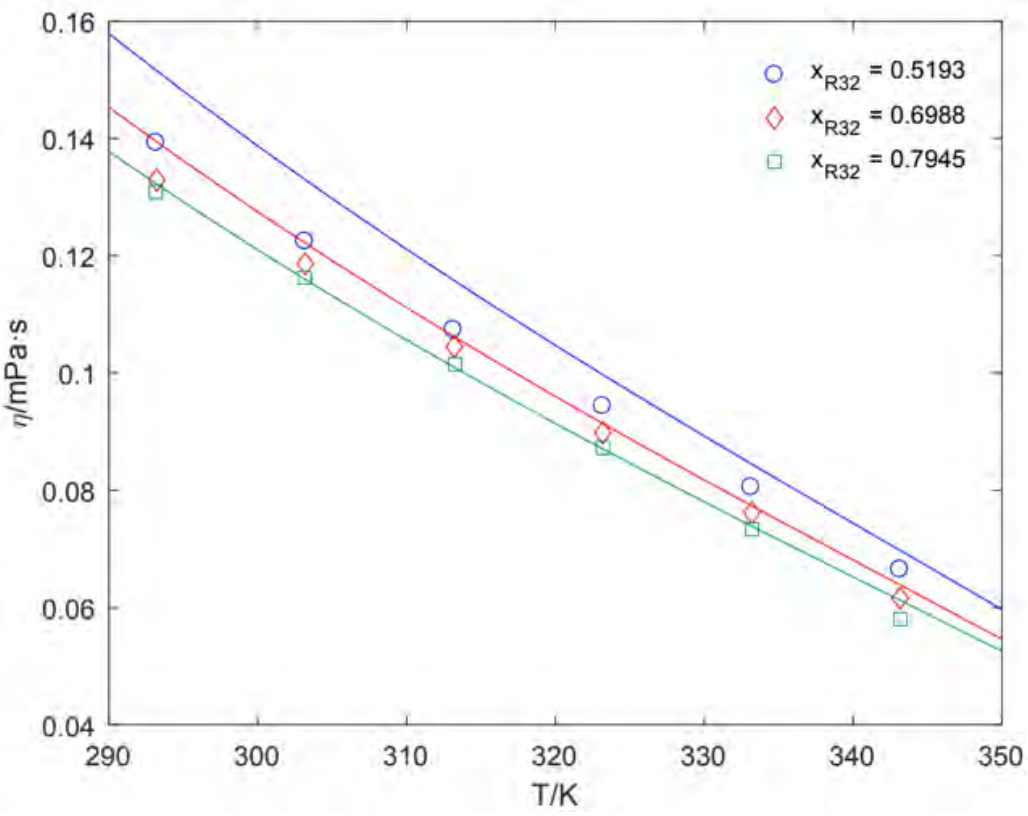

Figure 7: Albà et al.

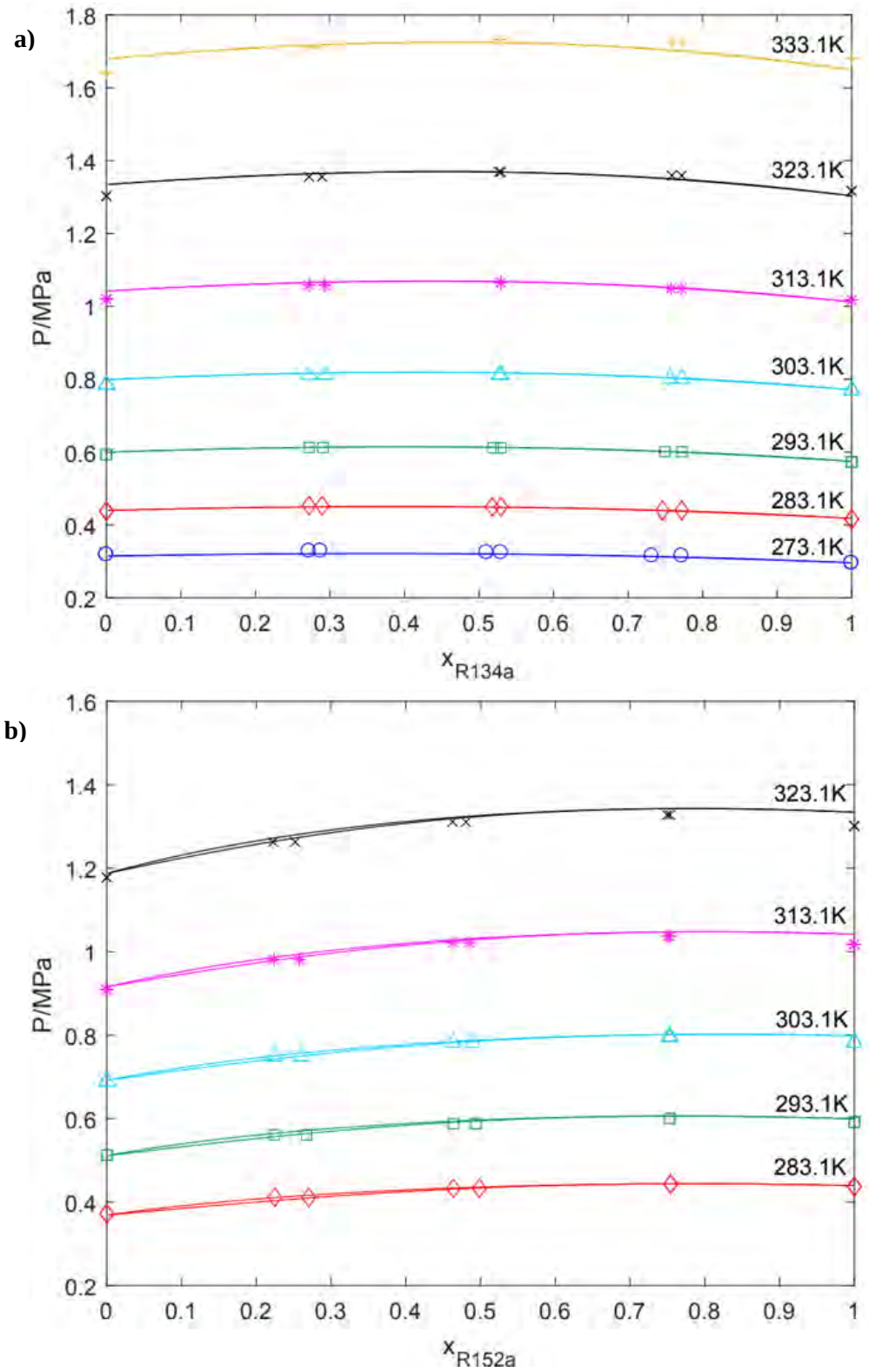

Figure 8: Albà et al.

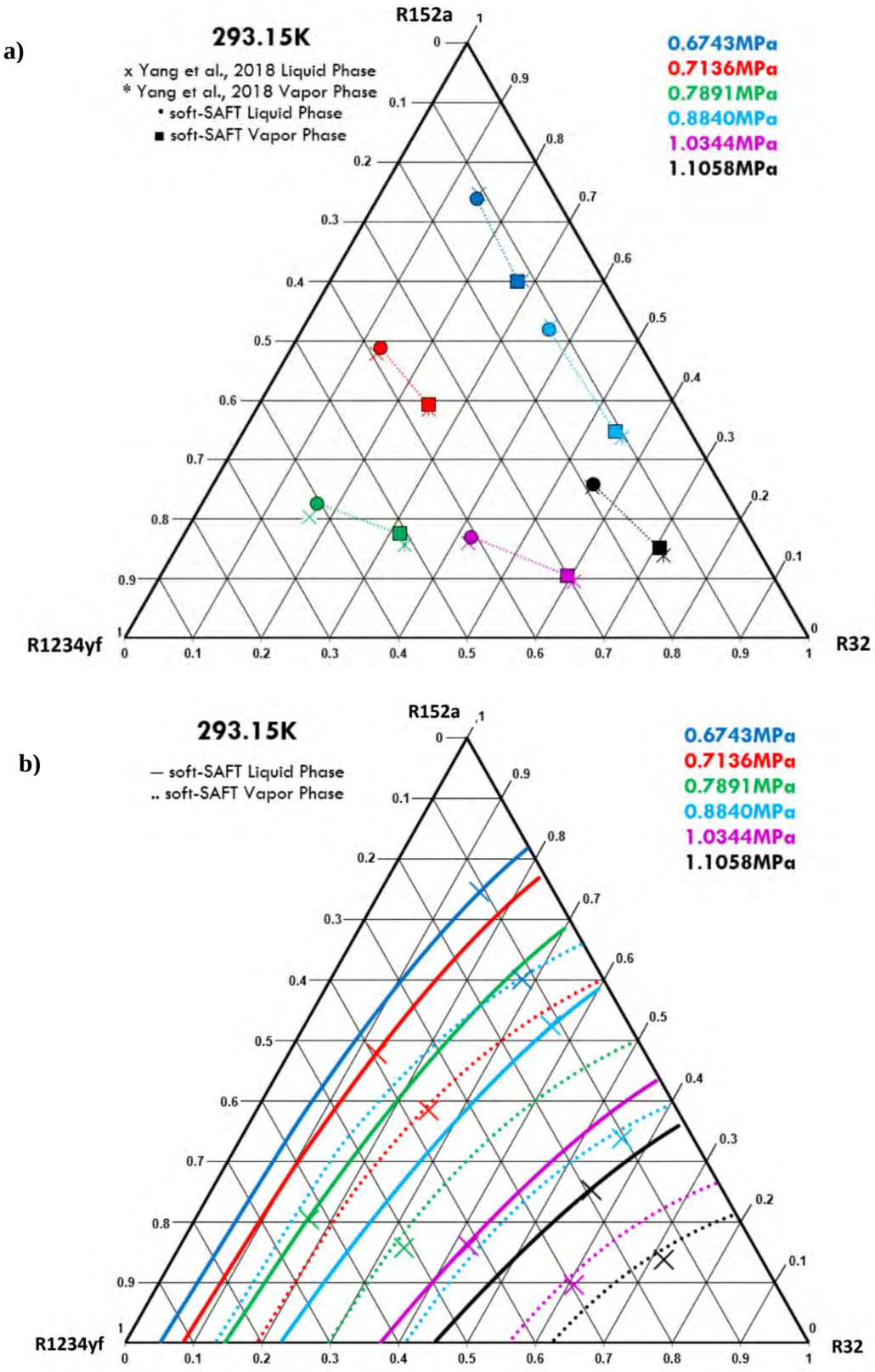

Figure 9: Albà et al.

This is a post-print (draft post-refereeing). Published in final edited form as
Alba, Carlos G.; Vega, Lourdes F.; Llovell, Felix. A consistent thermodynamic molecular model of n-hydrofluoroolefins and blends for refrigeration applications. En: *International Journal of Refrigeration-Revue Internationale du Froid*. (May 2020) Vol.113, p.145-155. Disponible a: https://doi.org/10.1016/j.ijrefrig.2020.01.008

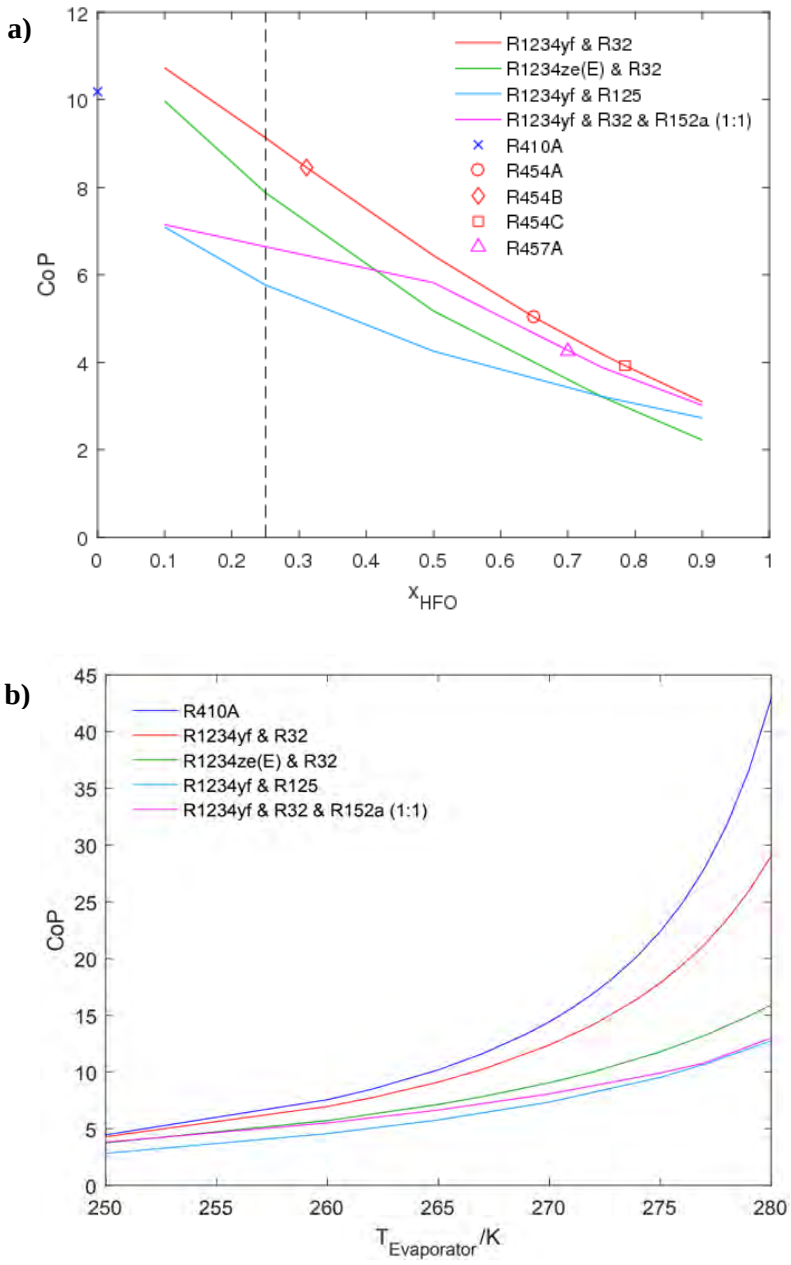

Figure 10: Albà et al.